Available online at www.sciencedirect.com

ScienceDirect

Solar Energy 130 (2016) 139–147

SOLAR ENERGY

www.elsevier.com/locate/solener

Tabulated values of the Shockley–Queisser limit for single junction solar cells

Sven Rühle

Solar Energy Consulting, Tel Aviv 62095, Israel

Received 8 October 2015; received in revised form 1 February 2016; accepted 8 February 2016
Available online 27 February 2016

Communicated by: Associate Editor Frank A. Nüesch

Abstract

The detailed balance limit for solar cells presented by Shockley and Queisser in 1961 describes the ultimate efficiency of an ideal *p–n* junction solar cell illuminated by a black body with a surface temperature of 6000 K. Today the AM 1.5G spectrum is the standard spectrum for non-concentrated photovoltaic conversion, taking light absorption and scattering in the atmosphere into account. New photovoltaic materials are investigated every day, but tabulated values to estimate their performance limits are difficult to find. Here values of the maximum short circuit current density (J_{sc}), open circuit voltage (V_{oc}), light to electric power conversion efficiency (η) as well as current density (J_{mpp}) and voltage (V_{mpp}) at the maximum power point are presented as a function of the light absorbers' band gap energy.

Keywords: Maximum photovoltaic conversion efficiency; Detailed-balance limit; ASTM G173-03; AM 1.5G; Standard conditions

1. Introduction

The maximum light to electric power conversion efficiency η of a single junction solar cell for a given illumination spectrum is known as detailed balance limit or Shockley–Queisser limit. Based on detailed balance considerations William Shockley and Hans-Joachim Queisser presented in 1961 for the first time the calculation of the maximum conversion efficiency of a *p–n* junction solar cell illuminated by the sun, where the sun spectrum was approximated by the emission of a black body with a surface temperature of $T_s = 6000$ K (Shockley and Queisser, 1961). They assumed that in an ideal solar cell the only recombination path which cannot be reduced to zero is radiative recombination, which defines the upper limit for the minority carrier lifetime (Queisser, 2009). For the generation of electron–hole pairs it was assumed that photons with an energy below the energy band gap do not interact with the solar cell while photons with an energy above the band gap are converted into electron-hole pairs with a quantum efficiency of 100%. Shockley and Queissers calculated the efficiency limit for a single junction solar cell at a cell temperature of $T_c = 300$ K.

Today the sun spectrum on earth is defined by the American Society for Testing and Materials (ASTM International Standard), which defines in the document ASTM G173-03 two terrestrial spectral irradiance distributions, the 'direct normal' and 'hemispherical on 37° tilted surface' (ASTM G173-03), which will be abbreviated as AM 1.5D and AM 1.5G throughout this article. Both

E-mail address: sven.ruhle@solarenergy-consulting.com
URL: http://www.solarenergy-consulting.com

http://dx.doi.org/10.1016/j.solener.2016.02.015
0038-092X/

terrestrial solar spectral irradiance distributions are shown in Fig. 1 together with the extraterrestrial irradiance distribution AM 0 just outside the earths atmosphere, where AM is the abbreviation for air mass and is defined by $1/\cos(\theta)$. Furthermore, the black body spectrum is shown that was used by Shockley and Queisser in their original work. The AM 1.5D spectrum is relevant for solar conversion systems based on light concentration with mirrors or lenses because it consists only the direct sunlight while the AM 1.5G spectrum includes also scattered light from the atmosphere and is relevant for PV systems without light concentration. Further details about their exact definition can be found elsewhere (Reference Solar Spectral Irradiance). The integrated power density is 900.1 W/m^2 for AM 1.5D and 1000.4 W/m^2 for the AM 1.5G spectral irradiance, which is substantially lower compared to 1576.7 W/m^2 corresponding to Shockley and Queissers approximation of the sun as a black body with a surface temperature of 6000 K. The ASTM G173 standard was adopted in January 2003 and has replaced the previous standard ASTM G159.

This work presents the theoretical maximum limit of the solar cell parameters (J_{sc}, V_{oc}, η, etc.) of single junction photovoltaic (PV) cells as a function of the band gap

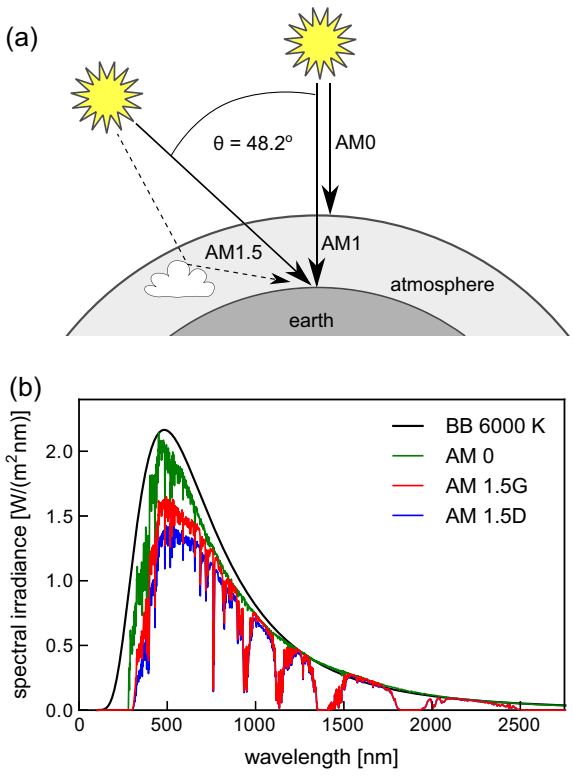

Fig. 1. (a) Schematic representation of the spectral irradiance outside the earths atmosphere (AM 0) and on the earths surface for direct sunlight shown by a solid arrow (AM 1.5D) and the direct sunlight together with the scattered contribution from atmosphere (solid and dashed arrow) integrated over a hemisphere (AM 1.5G). (b) Spectral irradiance according to ASTM G173-03 in comparison to the spectrum used by Shockley and Queisser of a black body with a surface temperature of 6000 K (BB 6000 K).

energy of the light absorber under illumination with the AM 1.5G spectrum and a solar cell temperature of 298.15 K (25 °C), corresponding to standard solar cell test conditions (Taylor et al., 2010). The maximum light to electric power conversion efficiency for AM 1.5G illumination, based on Shockley and Queissers detailed balance considerations is 33.16% and requires a semiconductor band gap of 1.34 eV (928 nm). Small deviations from this value can be found in the literature which might origin from a different standard spectrum which was used before the year 2003, a different cell temperature (e.g. 300 K), a different cell configuration including a reflector at the back side or from different numerical methods (Brown and Green, 2002; Peter, 2011; Ruppel and Wurfel, 1980; Kirchartz and Rau, 2008; Levy and Honsberg, 2006; ten Kate et al., 2013; Green et al., 2011; Thomas et al., 2012). Photovoltaic (PV) systems which can reach higher light to electric power conversion efficiencies beyond the single junction detailed balance limit are often referred to as 3rd or 4th generation PV. Even though detailed balance theory has been applied to a number of PV systems such as cells with light trapping (Yablonovitch and Miller, 2010), excitonic solar cells (Kirchartz et al., 2008), organic bulk heterojunction solar cells (Kirchartz et al., 2009), molecular PV devices (Nelson et al., 2004), thermophotovoltaic solar energy conversion (Harder and Würfel, 2003), multi-junction PV cells (De Vos, 2000), or quantum well solar cells (Barnham et al., 2002) up to now there are no tabulated values available for single junction solar cells that cover the spectral range from IR to UV. This information is of particular interest to estimate the performance limit of existing (Nayak and Cahen, 2014; Nayak et al., 2011) and novel photovoltaic materials based on the optical absorption onset like organo-metal halide perovskites (Kojima et al., 2009), quantum dot (Rühle et al., 2010), polymer (Helgesen et al., 2010) or metal oxide based solar cells (Rühle et al., 2012) and it shows to which extent existing photovoltaic absorbers can be improved until they reach their theoretical limit.

2. Calculations

For the calculation of the maximum photocurrent density J_{max} the AM 1.5G spectral irradiance was converted into an incident spectral photon flux ϕ^i according to

$$\phi^i = \frac{q\lambda}{hc}\mathrm{AM\,1.5G} \tag{1}$$

with the elementary charge q, the vacuum wavelength λ, the Planck constant h and the vacuum speed of light c. J_{max} was calculated by integration the spectral photon flux ϕ of the AM 1.5G irradiance from the band gap energy E_g up to the UV edge of 280 nm (4.43 eV), which is the shortest reported wavelength in the ASTM G173-03 standard:

$$J_{max}(E_g) = \int_0^\infty a(E)\,\phi^i(E)dE = \int_{E_g}^\infty \phi^i(E)dE \tag{2}$$

with the absorptance $a(E)$, which in an ideal case is one for photon energies equal or larger than the bandgap energy E_g ($E \geqslant E_g$) and zero for $E < E_g$.

Radiative recombination was calculated according to Kirchartz and Rau (2008) by using Würfel (1982) generalized Planck law (Planck, 1900) together with Kirchhoffs law (Kirchhoff, 1860), leading to an emitted photon flux ϕ^e as a function of an external applied voltage assuming flat quasi-Fermi levels

$$\phi^e(E,V) = \frac{2\pi E^2}{h^3c^2}\frac{a(E)}{\left[e^{\frac{E-qV}{k_B T_c}}-1\right]} \tag{3}$$

with the photon energy E, the external applied voltage V corresponding to the quasi-Fermi level splitting, the Boltzmann constant k_B and the solar cell temperature T_c. From this the radiative recombination current density J_r was calculated according to

$$\begin{aligned} J_r(E_g,V) &= f_g q\int_0^\infty \frac{2\pi E^2}{h^3c^2}\frac{a(E)}{\left[e^{\frac{E-qV}{k_B T_c}}-1\right]}dE \\ &= f_g q\int_{E_g}^\infty \frac{2\pi E^2}{h^3c^2}\frac{1}{\left[e^{\frac{E-qV}{k_B T_c}}-1\right]}dE \end{aligned} \tag{4}$$

where f_g is a geometrical factor (Fig. 2). Shockley and Queisser assumed that the solar cell is emitting radiation from the front and rear side ($f_g = 2$) and this assumption was used here.

Slightly higher conversion efficiencies can be reached when a perfect back reflector (Martí and Araújo, 1996) is placed onto the rear side of the cell such that radiation losses into one hemisphere are suppressed ($f_g = 1$) and results for this configuration are presented in the Supporting Information. In the following it will not be explicitly written that the currently densities are a function of the bandgap energy, i.e. $J_r(E_g, V) = J_r(V)$.

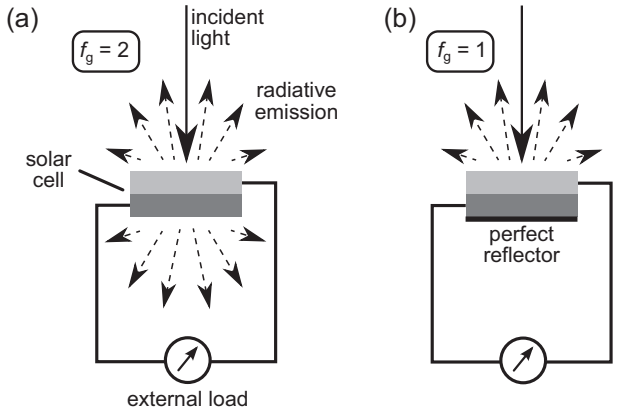

Fig. 2. Schematic drawing of a solar cell exposed to sun light from the top side (solid arrow). (a) The cell at temperature T_c and voltage V is emitting photons through its top and bottom (front and rear side) according to Eq. (4) (divided by q) with $f_g = 2$. (b) A perfect reflector prevents light emission from the bottom (rear) side of the solar cell ($f_g = 1$), leading to slightly higher conversion efficiencies as presented in the Supporting Information.

Following the original work of Shockley and Queisser (1961) non-radiative recombination and generation processes are represented by $J_{nr}(V)$ and $J_{nr}(0)$, respectively, which are identical for $V = 0$. For the calculation of the detailed balance limit non-radiative processes are negligible, however at the end of this work non-radiative processes are considered. At steady state the external current density J_{ext} has to be equal to the sum of all current densities in the cell

$$J_{ext} = J_{max} - J_r(V) + J_{nr}(0) - J_{nr}(V) \tag{5a}$$

$$J_{ext} = J_{max} - J_r(0) + [J_r(0) - J_r(V) + J_{nr}(0) - J_{nr}(V)] \tag{5b}$$

The expression in the square brackets represents a solar cell that is entirely surrounded by a black body at temperature T_c while the short circuit current density corresponds to the generation of electron hole pairs by incident sunlight (J_{max}) from which thermal recombination at zero bias ($J_r(0)$) has to be subtracted

$$J_{sc} = J_{max} - J_r(0) \tag{6}$$

To describe the current–voltage characteristics of the cell the parameter f_c was introduced to describe the fraction of radiative generation and recombination current densities.

$$J_r(0) - J_r(V) = f_c[J_r(0) - J_r(V) + J_{nr}(0) - J_{nr}(V)] \tag{7}$$

It was assumed that f_c is voltage independent. For the calculation of the detailed balance limit $f_c = 1$, which means that $J_{nr}(0) = J_{nr}(V) = 0$. The V_{oc} was calculated according to

$$V_{oc} = \min|J_{ext}(V)|. \tag{8}$$

The maximum power point voltage was calculated according to

$$V_{mpp} = \max(V \cdot J_{ext}(V)) \tag{9}$$

and the J_{mpp} was calculated according to

$$J_{mpp} = J_{max} - J_r(V_{mpp}) \tag{10}$$

The fill factor is defined as

$$FF = \frac{V_{mpp}\,J_{mpp}}{V_{oc}\,J_{sc}} \tag{11}$$

The light to electric power conversion efficiency η was calculated according to

$$\eta = \frac{V_{mpp}\,J_{mpp}}{\Phi^{AM\,1.5G}} \tag{12}$$

where $\Phi^{AM\ 1.5G}$ is the integrated spectral irradiance with a power density of 1000.37 W/m^2.

The black body irradiance that would correspond to a sun surface with a temperature of 6000 K measured at the sun–earth distance was calculated according to

$$L^{sun}(\lambda) = f_\omega \frac{2\pi hc^2}{\lambda^5}\frac{1}{\left[e^{\frac{hc}{\lambda k_B T_s}}-1\right]} \tag{13}$$

where f_ω is a geometrical factor that takes the limited angle into account from which solar radiation is falling onto the solar cell

$$f_\omega = \left(\frac{R_{\text{sun}}}{D_{\text{sun–earth}}}\right)^2 \tag{14}$$

The sun radius is $R_{\text{sun}} = 6.96 \cdot 10^8$ m and the distance between sun and earth is $D_{\text{sun–earth}} = 1.496 \cdot 10^{11}$ m. The black body irradiance L^{sun} was converted into an incident spectral photon flux according to Eq. (1) and the corresponding generation current density J_{max} was calculated according to Eq. (2). All calculations were performed in Python.

3. Results

3.1. The Shockley–Queisser limit for AM 1.5G and $T_c = 298.15$ K

The following discussion is considering a solar cell which is emitting radiation from its front and rear side as shown in Fig. 2a in accordance to the original work of Shockley and Queisser. Tabulated data of a cell with a perfect reflector at its rear side as schematically shown in Fig. 2b are presented in the Supporting Information. The maximum photocurrent densities as a function of the light absorber band gap are shown in Fig. 3. J_{max} is the calculated maximum electron–hole generation current density according to Eq. (2), for which it was assumed that only photons with an energy above the bandgap generate electron hole pairs with a quantum efficiency of 100%, while photons with lower energy do not interact with the solar cell. Reflection losses as well as more complex mechanisms such as up-conversion (Trupke et al., 2002a), down-conversion (Trupke et al., 2002b), multiple electron–hole pair generation (Nozik et al., 2010), or intermediate band assisted effects (Luque and Martí, 2010) were not taken into account. For the calculation of the short circuit current density J_{sc} the recombination current density at zero applied bias was subtracted from J_{max} (Eq. (6)). Both current densities are strongly increasing in the visible range, followed by a number of plateaus that correspond to gaps in the spectral irradiance distribution due to absorption and scattering in the earths atmosphere (Fig. 1). The difference between J_{max} and J_{sc} becomes only apparent at bandgap energies below 0.5 eV and does not exceed a few per mille as can be seen from Fig. 3c where J_{sc} divided by J_{max} is shown as a function of the band gap energy. It should be noted that in the literature often no distinction is made between J_{max} and J_{sc}, due to the extremely small differences in the visible range. Fig. 3 shows furthermore the current density at the maximum power point J_{mpp} for a solar cell that operates at the highest conversion efficiency at a given band gap. J_{mpp} is not constantly increasing with decreasing band gap energy in contrast to J_{sc} and shows a maximum at 2445 nm or 0.51 eV, due to the increase of the recombination current with decreasing band gap.

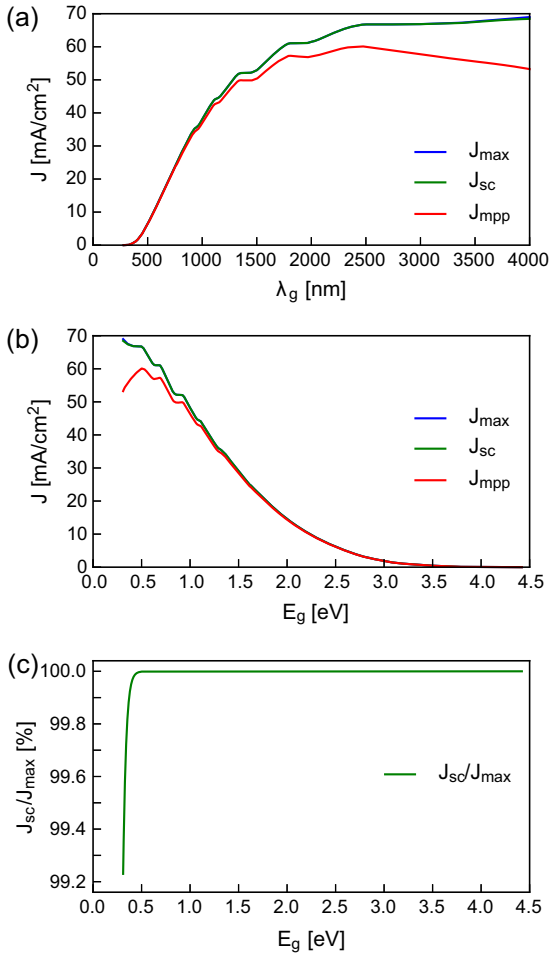

Fig. 3. The maximum electron–hole generation current density J_{max}, the short circuit current density J_{sc}, and the current density at the maximum power point J_{mpp} calculated for the AM 1.5G spectral irradiance as a function of (a) the band gap wavelength and (b) the band gap energy. (c) J_{sc} divided by J_{max} showing a small deviation of J_{sc} from J_{max} for band gap energies below 0.5 eV.

For a solar cell with a given band gap energy J_{sc} is the maximum current density that can be reached when each photon generates only one electron–hole pair. Higher reported current densities might be an indication for non-linear effects like multiple electron–hole generation, however often an incorrectly calibrated solar simulator or small cell areas that enhance edge effects are the more likely origin.

Fig. 4 shows the maximum open circuit voltage (V_{oc}) and the photovoltage at the maximum power point (V_{mpp}) as a function of the band gap wavelength and energy together with the bandgap potential E_g/q. With increasing band gap energy the V_{oc} and V_{mpp} are increasing even though the generation current density J_{max} is decreasing with increasing gap. The radiative recombination current depends on the electron and hole densities in the conduction and valence band, respectively, and these densities are described by energy difference between the electron quasi-Fermi level with the conduction band edge and the hole-quasi Fermi level with the valence band edge. For

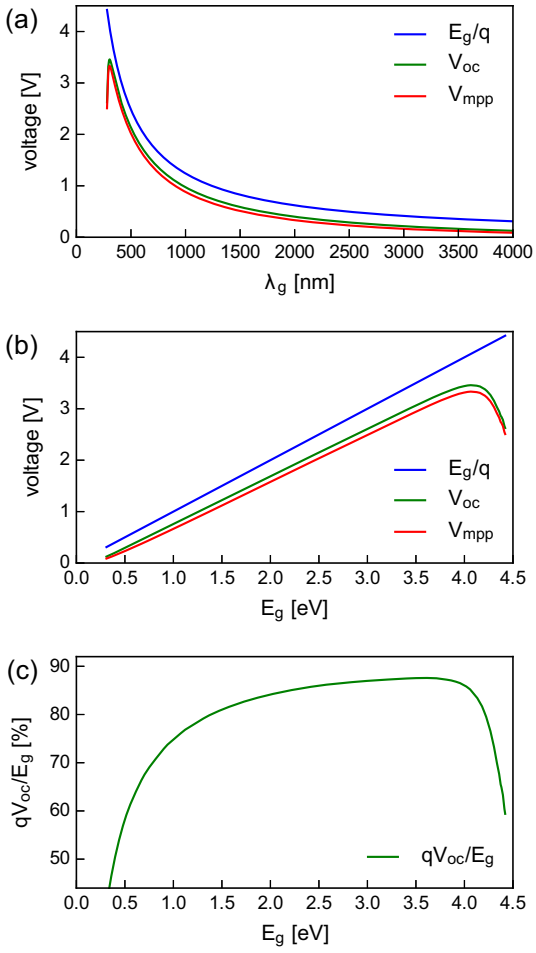

Fig. 4. Band gap potential E_g/q, open circuit voltage V_{oc} and maximum power point voltage as a function of (a) the band gap wavelength and (b) band gap energy. (c) Ratio of the V_{oc} vs the band gap potential.

detailed balance calculations it is assumed that the electron and hole conductivities are sufficiently high that the quasi-Fermi levels are flat and that the external applied voltage describes the quasi-Fermi level splitting in the cell. At open circuit the entire current density generated by photon absorption is recombining, leading to a quasi-Fermi level splitting described by the V_{oc}. With increasing band gap less electron–hole pairs are generated (see Fig. 3), causing lower charge carrier densities in the bands, which leads to a larger energy difference between the quasi-Fermi levels and the band edges. Thus with increasing band gap the V_{oc} is increasing with a lower slope compared to the band gap potential E_g/q (Fig. 4b).

In the UV the electron–hole generation current density (J_{sc}) is decreasing toward zero generating only a very low quasi-Fermi level splitting that is declining with increasing band gap. For the AM 1.5G spectral irradiance a maximum of the V_{oc} of 3.46 V is reached at a band gap of 4.06 eV (305 nm). The quasi-Fermi level splitting at the maximum power point (V_{mpp}) shows a very similar behavior.

The ratio of the V_{oc} divided by the band gap potential is shown in Fig. 4c, which describes the splitting of the electron and hole quasi Fermi levels relative to the band gap. At band gap energies between 0.31 and 1.00 eV the V_{oc} is increasing from 40% to 75% of the band gap potential; throughout the visible range the qV_{oc}/E_g is increasing further until a maximum of 87% is reached at $E_g = 3.6$ eV before the ratio starts decreasing in the UV spectral region. The ratio shows that the electron–hole pairs are more efficiently converted into electric energy at larger band gaps (<4 eV).

The theoretically maximum light to electric power conversion efficiency η for single junction solar cells (Shockley–Queisser limit) calculated for the AM 1.5G spectral irradiance according to ASTM G173-03 is shown in Fig. 5, together with certified record efficiencies of lab sized PV cells (area $\geqslant 1$ cm^2), taken from the Solar Cell Efficiency Tables (Green et al., 2016). The efficiency curve is not totally smooth due to atmospheric absorption bands at around 900, 1150, 1400, 1800 and 2500 nm and shows two local maxima of 32.85% at 1.15 eV (1080 nm) and 33.16% at 1.34 eV (928 nm). Comparison with Fig. 3 shows that the highest conversion efficiencies are achieved for band gaps where approximately half of the photons are not absorbed by the light absorber, e.g. $J_{max} = 30$–45 mA/cm^2. The solar cell parameters of record cells relative to the detailed balance values are discussed in more detail in Fig. 7.

It is furthermore interesting to look at the fill factor of a solar cell that is operated at its highest conversion efficiency,

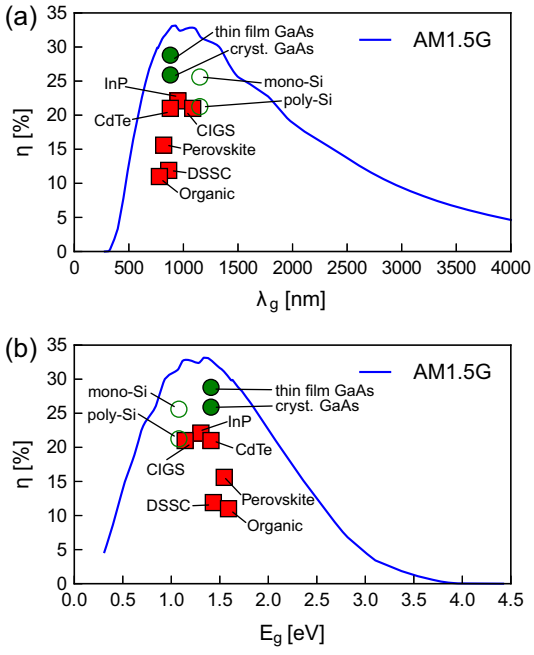

Fig. 5. The maximum light to electric power conversion efficiency (detailed balance limit) for a solar cell operated at 298.15 K and illuminated with the AM 1.5G spectral irradiance (ASTM 173-03) in accordance with standard solar test conditions as a function of (a) the band gap wavelength and (b) the band gap energy. Record efficiencies of laboratory cells differentiating between homo-junction (circles) and hetero-junction devices (squares) with indirect band gap (empty symbols) and absorbers with direct optical transitions (full symbols).

shown in Fig. 6. For band gap wavelengths below 800 nm the fill factor of a perfect solar cell is above 90% and is linearly decreasing with increasing band gap wavelength. Especially at low band gap energies below 1 eV the fill factor is dropping from above 85% down to below 60% leading to a worse conversion efficiency of electrons and holes into electric energy. It should be noted that for a given band gap energy the J_{sc}, V_{oc} and η are the maximum values which can only be reached when the solar cell is operated at the detailed balance limit. In contrast to that the fill factor can reach higher values than the reported ones when the cell is operated at conversion efficiencies below the detailed balance limit. On first sight that might seem surprising, but it becomes obvious when one recalls that the fill factor is only a relative measure between the voltage and current density at the maximum power point relative to the open- and short circuit values, respectively. Thus a solar cell with a given band gap operated at V_{oc} and/or a J_{sc} below the detailed balance limit can show a fill factor beyond the one shown in Fig. 6. This happens especially when the V_{mpp} and/or J_{mpp} do not differ much from V_{oc} and J_{sc}, respectively. However, in such case the overall conversion efficiency η will remain below the detailed balance limit.

All solar cell parameters for the Shockley–Queisser limit based on detailed balance considerations are summarized in Table 1 for band gap energies from 0.4 to 4.4 eV in steps of 100 meV. The highest efficiency of 33.16% is reached at a band gap energy of 1.34 eV, assuming radiative losses from the front and rear side of the solar cell (Fig. 2a). If a perfect reflector prevents emission from the rear side of the cell (Fig. 2b), then a conversion efficiency of 33.77% at the same band gap energy can be reached. Solar cell parameters for both configurations using band gap energies in 10 meV steps are presented in the Supporting Information.

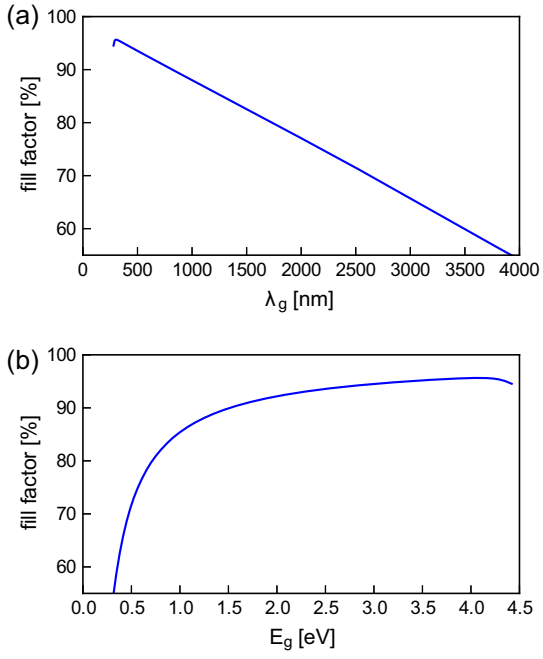

Fig. 6. The fill factor at the detailed balance limit as a function of (a) the band gap wavelength and (b) the band gap energy.

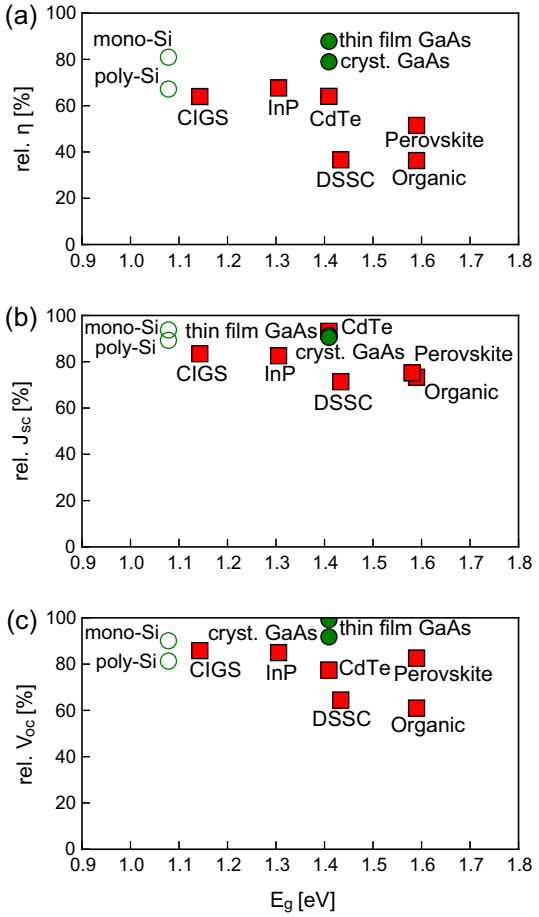

Fig. 7. Solar cell parameters of record efficiency cells relative to the detailed balance limit. (a) Conversion efficiency, (b) short circuit current density and (c) open circuit voltage. Homo-junction cells are shown as round circles while hetero-junctions are shown as squares. Full symbols are used for direct band gap absorbers while empty symbols are used for indirect band gap cells.

3.2. Record cell efficiencies

Let us now have a look at the certified values of record PV cells (Green et al., 2016) and compare their parameters with the detailed balance limit. In Fig. 7 the conversion efficiency η, J_{sc} and V_{oc} are shown in percent relative to the detailed balance values as a function of their band gap energy. Band gap values were derived from the onset of the external quantum efficiency (EQE) published in the Solar Cell Efficiency Tables (Green et al., 2016), taking the value where the EQE is 10%. Homo-junction cells are shown by circles while hetero-junctions cells are represented by squares. Indirect band gap semiconductors have empty symbols while full symbols are used for light absorbers where the energetically lowest optical transition can be excited without the interaction of phonons like in direct

Table 1
Detailed balance limit for a single junction solar cell at a cell temperature of 25 °C illuminated by the AM 1.5G Spectral Irradiance (ASTM G173-03) assuming radiative emission from the front and rear side of the solar cell.

E_g (eV)	λ_g (nm)	J_{max} (mA/cm^2)	J_{sc} (mA/cm^2)	J_{mpp} (mA/cm^2)	V_{oc} (V)	V_{mpp} (V)	FF (%)	η (%)
0.4	3099.6	66.95	66.93	57.29	0.202	0.152	64.5	8.73
0.5	2479.7	66.75	66.74	60.08	0.291	0.232	71.7	13.94
0.6	2066.4	62.20	62.20	57.50	0.381	0.314	76.3	18.06
0.7	1771.2	60.70	60.70	57.04	0.472	0.400	79.6	22.81
0.8	1549.8	54.46	54.46	51.72	0.563	0.486	82.0	25.13
0.9	1377.6	52.06	52.06	49.84	0.656	0.575	83.9	28.64
1	1239.8	48.22	48.22	46.42	0.749	0.664	85.4	30.82
1.1	1127.1	44.23	44.23	42.77	0.842	0.754	86.6	32.23
1.2	1033.2	39.99	39.99	38.80	0.935	0.844	87.7	32.74
1.3	953.7	35.82	35.82	34.86	1.028	0.935	88.5	32.57
1.4	885.6	32.88	32.88	32.08	1.122	1.026	89.3	32.91
1.5	826.6	28.97	28.97	28.32	1.215	1.118	89.9	31.64
1.6	774.9	25.47	25.47	24.94	1.309	1.209	90.5	30.14
1.7	729.3	22.46	22.46	22.02	1.402	1.301	91.0	28.64
1.8	688.8	19.65	19.65	19.29	1.496	1.393	91.4	26.86
1.9	652.5	16.97	16.97	16.68	1.589	1.485	91.8	24.75
2	619.9	14.59	14.59	14.35	1.683	1.577	92.2	22.62
2.1	590.4	12.48	12.48	12.29	1.776	1.669	92.5	20.50
2.2	563.6	10.62	10.62	10.47	1.870	1.761	92.8	18.42
2.3	539.1	8.96	8.96	8.84	1.963	1.853	93.1	16.37
2.4	516.6	7.50	7.50	7.41	2.057	1.945	93.3	14.40
2.5	495.9	6.20	6.20	6.12	2.150	2.037	93.6	12.47
2.6	476.9	5.04	5.04	4.98	2.242	2.128	93.8	10.59
2.7	459.2	4.00	4.00	3.95	2.334	2.219	94.0	8.77
2.8	442.8	3.10	3.10	3.06	2.426	2.310	94.2	7.08
2.9	427.5	2.45	2.45	2.42	2.518	2.401	94.3	5.81
3	413.3	1.86	1.86	1.84	2.609	2.491	94.5	4.58
3.1	399.9	1.35	1.35	1.34	2.699	2.581	94.7	3.45
3.2	387.5	1.06	1.06	1.05	2.792	2.672	94.8	2.80
3.3	375.7	0.82	0.82	0.81	2.883	2.763	94.9	2.24
3.4	364.7	0.60	0.60	0.59	2.974	2.853	95.1	1.70
3.5	354.2	0.44	0.44	0.43	3.064	2.942	95.2	1.27
3.6	344.4	0.30	0.30	0.29	3.153	3.030	95.3	0.89
3.7	335.1	0.18	0.18	0.18	3.239	3.115	95.4	0.56
3.8	326.3	8.18E−02	8.18E−02	8.11E−02	3.317	3.193	95.5	0.26
3.9	317.9	2.82E−02	2.82E−02	2.80E−02	3.388	3.264	95.6	9.14E−02
4	310.0	4.67E−03	4.67E−03	4.64E−03	3.441	3.316	95.6	1.54E−02
4.1	302.4	1.66E−04	1.66E−04	1.65E−04	3.454	3.328	95.6	5.49E−04
4.2	295.2	3.44E−07	3.44E−07	3.41E−07	3.392	3.268	95.6	1.12E−06
4.3	288.3	1.44E−12	1.44E−12	1.43E−12	3.171	3.048	95.3	4.37E−12

band gap semiconductors, molecular dyes that are used as a light absorber in dye sensitized solar cells (DSSCs), or polymer light absorbers used in organic solar cells.

Looking at the relative efficiency one can see that thin film GaAs is reaching an efficiency of more than 80% of its detailed balance limit and can thus be considered as the best optimized solar cell, which is also reflected by high values in the relative J_{sc} and V_{oc}. Mono-crystalline Si as an indirect band gap semiconductor is the second best optimized solar cell, which reaches photocurrent densities close to its theoretical maximum and a high relative V_{oc}. Thus GaAs and Si which are both homo-junction solar cells are today the best optimized PV devices.

Hetero-junction solar cells can currently reach 36–68% of the efficiency of the detailed balance limit. Especially in DSSCs and organic solar cells the relatively low V_{oc} is limiting the conversion efficiency. In DSSCs the non-optimized energy levels of the dye with respect to the redox potential of the electrolyte are limiting the photovoltage while in organic PV cells an energy difference between the donor and acceptor is required to enable exciton dissociation, which comes on the account of the photovoltage. In tendency hetero-junction cells show larger voltage losses due to band edge discontinuities or non-optimized energy levels at the junction, leading to lower level of optimization compared to homo-junction devices. However, organo-metal halide perovskite solar cells can already reach a V_{oc} above 80% of its theoretical limit indicating nearly optimized energy levels at the hetero-junction, which is remarkable considering the short time these devices are under optimization so far. Besides the efficiency the performance stability of solar cells is an essential parameter for large scale application, which is not considered in these graphs.

3.3. The effect of recombination

Shockley and Queisser calculated the efficiency limit for a single junction solar cell based on the assumption that the sun spectrum can be approximated by black body radiation with a temperature of 6000 K. Furthermore, they assumed that the solar cell has a temperature of 300 K, which differs slightly from todays' standard test conditions of 298.15 K (25 °C). Fig. 8 shows the efficiency as function of the band gap energy (black line) with a maximum of 30.66% at a band gap energy of 1.32 eV, which differs slightly from the band gap value of 1.1 eV from Shockley and Queissers work. A reason for this could be that in this work the Bose–Einstein statistics $[\exp((E-qV)/k_BT_c)-1]^{-1}$ that appears in Eqs. (3) and (4) was numerically integrated and not approximated by a Boltzmann distribution. A comparison with the detailed balance limit for single junction cells under standard test conditions (AM 1.5G, 25 °C) reveals that higher conversion efficiencies can be reached with the AM 1.5G spectrum for band gap energies between 0.6 and 1.7 eV. At higher band gap energies illumination by the black body spectrum leads to higher conversion efficiencies, corresponding to a higher power density of the black body spectrum in this spectral range (see Fig. 1b). For this comparison one should keep in mind that the power density of the AM 1.5G irradiance is with 1000.4 W/m^2 substantially smaller than 1576.7 W/m^2 of the black body irradiance.

Furthermore the effect of non-radiative recombination is shown in Fig. 8. As proposed by Shockley and Queisser it was assumed that non-radiative recombination shows the same voltage dependence like radiative recombination such that a factor f_c could be introduced that describes the fraction of radiative recombination. If $f_c = 1$ then there are no non-radiative recombination paths and the calculated efficiency corresponds to the detailed balance limit, shown by the green curve (same data like in Fig. 5). For $f_c = 10^{-3}$ the recombination is by a factor of 1000 stronger and consists to 0.1% of radiative and 99.9% of non-radiative recombination and the maximum efficiency that can be reached is 27.3% at a band gap energy of 1.39 eV. If the recombination is a million times stronger ($f_c = 10^{-6}$) the maximum efficiency can still reach 21.7% at a band gap of 1.52 eV. One should note that window where the highest efficiencies can be reached (e.g. 90% of η_{max}) is moving toward higher band gap energies with increasing recombination. Auger recombination and Shockley–Read–Hall recombination are non-radiative processes, where the latter describes recombination associated to defects. Deriving defect densities based on the strength of the non-radiative recombination current density would be desirable but is not possible due to the unknown charge carrier life times which are also affecting the recombination rate.

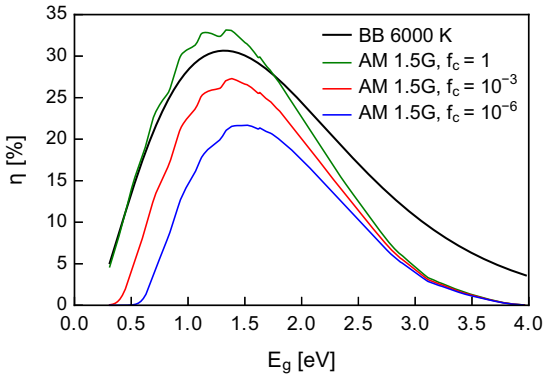

Fig. 8. Shockley–Queisser limit for a solar cell with a cell temperature of 300 K illuminated by a black body with a surface temperature of 6000 K (black curve) compared to the detailed balance limit for standard solar cell test conditions ($T_c = 298.15$ K, AM 1.5G) considering only radiative recombination (green curve, same data like in Fig. 5), non-radiative recombination that is 10^3 (red curve) and 10^6 (blue curve) times stronger than radiative recombination. (For interpretation of the references to color in this figure legend, the reader is referred to the web version of this article.)

For negligible non-radiative recombination the reported J_{max}, J_{sc}, V_{oc} and η are the highest possible values at a given band gap energy under AM 1.5G illumination according to ASTM G173-03 and a solar cell temperature of 298.15 K (25 °C). Exceeding these limits requires a more complex solar cell concept, labelled as 3rd or 4th generation photovoltaics that includes multi-junction devices, up- or down-conversion, multiple electron–hole pair generation, etc. From time to time publications make headlines by claiming efficiencies above the Shockley-Limit without pinpointing to advanced effects from 3rd/4th generation PV. Especially when it comes to the J_{sc} values close to or above the detailed balance limit are reported, which can be more often explained by an illumination source with a spectral irradiance that does not match well the AM 1.5G spectrum, a solar simulator that deteriorated from calibration or a too small solar cell area below 1cm^2, which is the minimum cell size to report efficiency values and to be listed in the solar cell efficiency tables. Especially for very small illuminated solar cell areas edge effects can become dominant to an extent that a meaningful normalization of the current with respect to the cell area is difficult or impossible.

4. Conclusions

This articles provides the maximum light to electric power conversion efficiency η, J_{max}, J_{sc}, J_{mpp}, V_{oc} and V_{mpp} for single junction solar cells as a function of the solar cell band gap in tabulated form. The calculations are based on illumination with the AM 1.5G spectrum according to ASTM G173-03 standard and a solar cell temperature of 25 °C. Conversion efficiencies above 30% can be reached for a solar cell band gap between 0.93 and 1.61 eV. In this range the V_{oc} can reach 0.69–1.31 V, corresponding to 74–82% of the band gap potential and a J_{sc} between 51.7 and 25.2 mA/cm^2. Non-radiative recombination which is 10^6 times stronger than radiative recombination is reducing the efficiency to 21.7% at a band gap of 1.52 eV.

Appendix A. Supplementary material

Supplementary data associated with this article can be found, in the online version, at http://dx.doi.org/10.1016/j.solener.2016.02.015.

References

ASTM International Standard, http://www.astm.org/.

ASTM G173-03, http://www.astm.org/Standards/G173.htm.

Barnham, K.W.J., Ballard, I., Connolly, J.P., Ekins-Duakes, N.J., Kluftinger, B.G., Nelson, J., et al., 2002. Quantum well solar cells. Phys. E 14, 27–36. http://dx.doi.org/10.1016/S0169-4332(96)00876-8.

Brown, A.S., Green, M.a., 2002. Detailed balance limit for the series constrained two terminal tandem solar cell. Phys. E Low-Dimens. Syst. Nanostruct. 14, 96–100. http://dx.doi.org/10.1016/S1386-9477(02)00364-8.

De Vos, A., 2000. Detailed balance limit of the efficiency of tandem solar cells. J. Phys. D. Appl. Phys. 13, 839–846. http://dx.doi.org/10.1088/0022-3727/13/5/018.

Green, M.A., Emery, K., Hishikawa, Y., Warta, W., 2011. Solar cell efficiency tables (version 37). Prog. Photovoltaics Res. Appl. 19, 84–92. http://dx.doi.org/10.1002/pip.1088.

Green, M.A., Emery, K., Hishikawa, Y., Warta, W., Dunlop, E.D., 2016. Solar cell efficiency tables (version 47). Prog. Photovoltaics Res. Appl. 24, 3–11. http://dx.doi.org/10.1002/pip.2728.

Harder, N., Würfel, P., 2003. Theoretical limits of thermophotovoltaic solar energy conversion. Semicond. Sci. Technol. 151, S151–S157. http://dx.doi.org/10.1088/0268-1242/18/5/303.

Helgesen, M., Søndergaard, R., Krebs, F.C., 2010. Advanced materials and processes for polymer solar cell devices. J. Mater. Chem. 20, 36–60. http://dx.doi.org/10.1039/B913168J.

Kirchartz, T., Rau, U., 2008. Detailed balance and reciprocity in solar cells. Phys. Status Solidi Appl. Mater. Sci. 205, 2737–2751. http://dx.doi.org/10.1002/pssa.200880458.

Kirchartz, T., Mattheis, J., Rau, U., 2008. Detailed balance theory of excitonic and bulk heterojunction solar cells. Phys. Rev. B. 78, 235320. http://dx.doi.org/10.1103/PhysRevB.78.235320.

Kirchartz, T., Taretto, K., Rau, U., 2009. Efficiency limits of organic bulk heterojunction solar cells. J. Phys. Chem. C. 113, 17958–17966. http://dx.doi.org/10.1021/jp906292h.

Kirchhoff, G., 1860. Ueber das Verhältnis zwischen dem Emissionsvermögen und dem Absorptionsvermögen der Körper für Wärme und Licht. Ann. Phys. Chemie. 109, 275.

Kojima, A., Teshima, K., Shirai, Y., Miyasaka, T., 2009. Organometal halide perovskites as visible-light sensitizers for photovoltaic cells. J. Am. Chem. Soc. 131, 6050–6051. http://dx.doi.org/10.1021/ja809598r.

Levy, M.Y., Honsberg, C., 2006. Rapid and precise calculations of energy and particle flux for detailed-balance photovoltaic applications. Solid State Electron. 50, 1400–1405. http://dx.doi.org/10.1016/j.sse.2006.06.017.

Luque, A., Martí, A., 2010. The intermediate band solar cell: progress toward the realization of an attractive concept. Adv. Mater. 22, 160–174. http://dx.doi.org/10.1002/adma.200902388.

Martí, A., Araújo, G.L., 1996. Limiting efficiencies for photovoltaic energy conversion in multigap systems. Sol. Energy Mater. Sol. Cells 43, 203–222. http://dx.doi.org/10.1016/0927-0248(96)00015-3.

Nayak, P.K., Cahen, D., 2014. Updated assessment of possibilities and limits for solar cells. Adv. Mater. 26, 1622–1628. http://dx.doi.org/10.1002/adma.201304620.

Nayak, P.K., Bisquert, J., Cahen, D., 2011. Assessing possibilities and limits for solar cells. Adv. Mater. 23, 2870–2876. http://dx.doi.org/10.1002/adma.201100877.

Nelson, J., Kirkpatrick, J., Ravirajan, P., 2004. Factors limiting the efficiency of molecular photovoltaic devices. Phys. Rev. B. 69, 1–11. http://dx.doi.org/10.1103/PhysRevB.69.035337.

Nozik, A.J., Beard, M.C., Luther, J.M., Law, M., Ellingson, R.J., Johnson, J.C., 2010. Semiconductor quantum dots and quantum dot arrays and applications of multiple exciton generation to third-generation photovoltaic solar cells. Chem. Rev. 110, 6873–6890. http://dx.doi.org/10.1021/cr900289f.

Peter, L.M., 2011. Towards sustainable photovoltaics: the search for new materials. Philos. Trans. R. Soc. A Math. Phys. Eng. Sci. 369, 1840–1856. http://dx.doi.org/10.1098/rsta.2010.0348.

Planck, M., 1900. Zur theorie des gesetzes der energieverteilung im normalspektrum. Verhandl. Der Dtsch. Phys. Gesellschaft. 2, 237–245.

Queisser, H.J., 2009. Detailed balance limit for solar cell efficiency. Mater. Sci. Eng. B 159–160, 322–328. http://dx.doi.org/10.1016/j.mseb.2008.06.033.

Reference Solar Spectral Irradiance: Air Mass 1.5, http://rredc.nrel.gov/solar/spectra/am1.5/.

Rühle, S., Shalom, M., Zaban, A., 2010. Quantum-dot-sensitized solar cells. ChemPhysChem 11, 2290–2304. http://dx.doi.org/10.1002/cphc.201000069.

Rühle, S., Anderson, A.Y., Barad, H.N., Kupfer, B., Bouhadana, Y., Rosh-Hodesh, E., et al., 2012. All-oxide photovoltaics. J. Phys. Chem. Lett. 3, 3755–3764. http://dx.doi.org/10.1021/jz3017039.

Ruppel, W., Wurfel, P., 1980. Upper limit for the conversion of solar energy. IEEE Trans. Electron Dev., 27–817 http://dx.doi.org/10.1109/T-ED.1980.19950.

Shockley, W., Queisser, H.J., 1961. Detailed balance limit of efficiency of p–n junction solar cells. J. Appl. Phys. 32, 510. http://dx.doi.org/10.1063/1.1736034.

Taylor, N., Dunlop, E., Fabero, F., Friesen, G., Herrmann, W., Hohl-Ebinger, J., et al., 2010. Guidelines for PV power measurement in industry. Ispra. http://dx.doi.org/10.2788/90247.

ten Kate, O.M., de Jong, M., Hintzen, H.T., van der Kolk, E., 2013. Efficiency enhancement calculations of state-of-the-art solar cells by luminescent layers with spectral shifting, quantum cutting, and quantum tripling function. J. Appl. Phys. 114, 084502. http://dx.doi.org/10.1063/1.4819237.

Thomas, C.P., Wedding, A.B., Martin, S.O., 2012. Theoretical enhancement of solar cell efficiency by the application of an ideal "down-shifting" thin film. Sol. Energy Mater. Sol. Cells 98, 455–464. http://dx.doi.org/10.1016/j.solmat.2011.11.027.

Trupke, T., Green, M.A., Würfel, P., 2002a. Improving solar cell efficiencies by up-conversion of sub-band-gap light. J. Appl. Phys. 92, 4117. http://dx.doi.org/10.1063/1.1505677.

Trupke, T., Green, M.A., Würfel, P., 2002b. Improving solar cell efficiencies by down-conversion of high-energy photons. J. Appl. Phys. 92, 1668. http://dx.doi.org/10.1063/1.1492021.

Würfel, P., 1982. The chemical potential of radiation. J. Phys. C Solid State Phys. 15, 3967–3985. http://dx.doi.org/10.1088/0022-3719/15/18/012.

Yablonovitch, E., Miller, O., 2010. The influence of the $4n^2$ light trapping factor on ultimate solar cell efficiency. Imag. Appl. Opt. Congr., SWA1 http://dx.doi.org/10.1364/OSE.2010.SWA1.